

Universality in the mechanics of soft Kirigami

Yukino Kako and Ko Okumura

Physics Department and Soft Matter Center,

Ochanomizu University, 2-1-1 Ohtsuka,

Bunkyo-ku, Tokyo 112-8610, Japan

Abstract

Recently, simple scaling laws concerning the mechanical response and mechanical transition of Kirigami have been revealed through agreement between theory and experiment for kirigami made of paper [M. Isobe and K. Okumura, *Sci. Rep.* 2016]. Here, we provide experimental data obtained from kirigami made of soft elastic sheets to demonstrate good agreement with previous theories, although a number of assumptions in the theory are violated and the elastic modulus is three orders of magnitude smaller in the present case. This remarkable universality in the mechanics of Kirigami, which could be useful for applications, is reported with physical insights based on previous theories.

I. INTRODUCTION

It has been widely known that simple patterning on sheets [1, 2], frequently motivated by Origami or Kirigami (Japanese traditional craft technique based on folding and/or cutting paper), could change them to mechanical metamaterials [3, 4] or tunable mechanical devices [5], exhibiting useful mechanical and functional properties. A simple kirigami structure is obtained by introducing a number of parallel cuts on a sheet. Such a simple structure gives the sheet a high extensibility, even for graphene sheets [6, 7]. The physical mechanism of this high stretchability was identified as the transition from the in-plane to out-of-plane deformation, which is accompanied by a buckling-induced rotation of each unit of the structure [8]. The buckling-induced rotation has been exploited for developing solar-tracking batteries [9] and dynamic shading systems [10]. Various other cut patterns have been studied to explore versatile possibilities of the application of kirigami [11, 12]. Frictional and interfacial properties of kirigami have been utilized for fabricating soft actuator [13] and enhancing film adhesion [14], respectively. However, high stretchability of kirigami remains one of the important properties of kirigami and has been exploited in various applications, which include conducting nanocomposites [15], piezoelectric materials [16], metallic glass [17], thermally responsive materials [18], stretchable strain sensor [19] and flexible film bioprobe [20].

Although applications have widely been studied, the basic physical understanding of the high extensibility of kirigami is still premature.

Here, we investigate mechanical response of a simple kirigami structure fabricated with sheets of soft elastic foam and surprisingly find that their characteristics can be well captured by previous theories [8, 21, 22] although a number of assumptions in them are violated and the elastic modulus is three orders of magnitude smaller in the present case. This unexpected universality in the mechanics of kirigami is interpreted in the light of previous theories.

II. EXPERIMENTAL

As in our previous study [8, 21, 22], we focus on a simple kirigami structure, characterized by three parameters, thickness h and geometrical parameters d , w , and N (fixed to $N = 10$, throughout the present study), as illustrated in Fig. 1 (a). The structure is composed of N elemental units (width $w + 2d$ and height $2d$) connected at the top and bottom in the

central area of width d . An elemental unit is composed of two thin strips of height d , each of which will be called a half element, connected at both lateral ends with regions of width d . We assign the unit element number n to each element, from $n = 1$ (for the bottom unit) to $n = N$ (for the top).

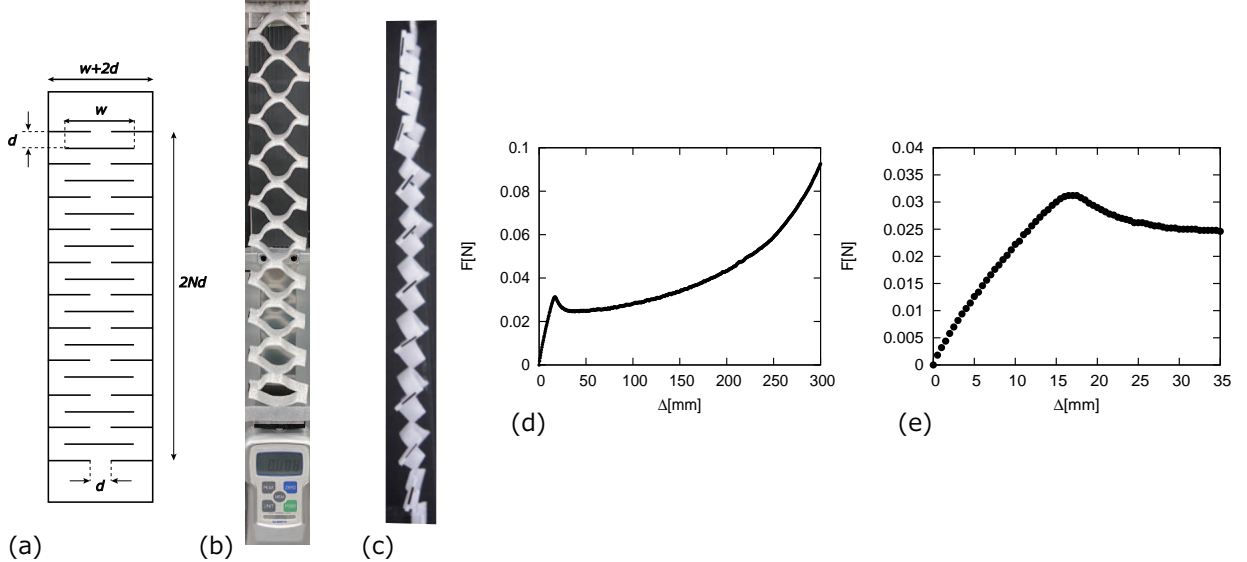


FIG. 1: (a) Geometry of kirigami, with the definition of kirigami parameters d and w (with $N = 10$ throughout this study). (b) Front view of highly extend kirigami made of soft elastic sheet at a strain 0.825. (c) Side view at a strain 0.4. (d) Force F vs extension Δ obtained for a kirigami sample. (e) Magnified plot of the initial regime in (d). (b) and (c) correspond to $(h, d, w) = (2, 10, 50)$ in mm, while (d) and (e) to $(2.5, 12, 70)$.

This structure is made of soft elastic sheets, commercially sold for shock-absorbing purposes (Lightron S, Sekisui Chemical Co., Ltd.). This material is linear elastic for small deformation up to a strain $\varepsilon \simeq 0.1$ with an elastic modulus $E \simeq$ a few MPa, which is three orders of magnitude smaller than that of paper (fracture mechanical properties for this material have been studied in [23–25]). In the present experiment, we use two types of sheets: one with $h = 2.0$ mm and the other with 2.5 mm, of which Young’s moduli are respectively 2.13 ± 0.18 and 1.14 ± 0.01 MPa. The structure was created using a commercial cutting plotter (silhouette CAMEO 3, Graphtech Corp.) with a special blade (SILH-BLADE-DEP, Graphtech Corp.). The parameters d and w are in the ranges, 3 to 14 mm and 30 to 70 mm, respectively, where w is always at least 5 times as large as d . This is because previous theory is justified in the limit $w \gg d$ and was confirmed to be practically valid when w was 5 times as large as d for kirigami made of paper [8].

This sample was stretched using a slider system (EZSM6D040, Oriental Motor) with a low speed (0.5 mm/s), as in Fig. 1 (b). In Fig. 1 (c), we see elements rotating to achieve an out-of-plane deformation, where rotations are visible through black short lines corresponding to side edges (height $2d$) of elemental units. Note here that the rotation angle is not homogeneous. Even the direction of the rotation is not the same for N elements! As seen in Fig. 1 (c), the direction in the middle area is opposite to the one in the top and bottom area. Note that this inhomogeneity is not reflected in the previous theories [8, 22].

III. RESULTS

A. Two types of experiment and their features

The profile of the force-extension curve obtained for new samples was not well reproducible, as shown in Fig. 2 (a). This may be because of a slightly wavy texture (the wave length and amplitude \simeq cm and mm, respectively) of the sheet surface created in the fabrication process (we introduce the kirigami structure to sheets so that the cuts run perpendicular to the direction of the wave vector and thus stretched kirigami in the wave direction). However, as shown in Fig. 2 (b), if we reused an already-extended sample after flattening it with a protocol specified below, we could obtain well-reproducible curve profiles for the second to (at least) fifth extensions. In addition, the averaged plot obtained from the used sample was nearly independent of samples, if the parameters h , d , and w were the same, as demonstrated in Fig. 2 (c).

The protocol for the used-sample experiment is as follows. (1) Each extension experiment, we stretch the sample to an extension $\Delta = \Delta_b/2$ and keep the extension for three minutes. (2) We flatten the sample with a book (width 17.8 cm, height 25.3 cm, and weight 452.6 g) for 15 minutes with keeping $\Delta = 0$ to restart the next stretch. In the above, $\Delta_b = 2Nd \left(\sqrt{1 + (w/d - 1)^2} - 1 \right)$ is a measure of extension, at which each element starts breaking when all elements are stretched homogeneously.

Even after thus-explained flattening for relaxation, a used sample before stretching is not flat anymore. All elements are already rotated slightly, typically less than a few degrees, in the same direction (but with practically negligible initial elongation on the scale of measurement). This implies that there is no in-plane to out-of-plane transition in used samples

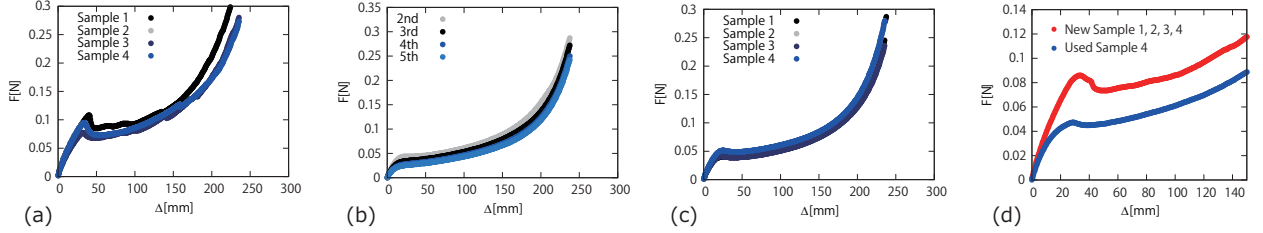


FIG. 2: (a) F vs Δ obtained for four new samples of kirigami, showing a low profile-reproducibility. (b) F vs Δ obtained from the second to fifth tensile experiments using an already-extended sample, with each performed after flattening for relaxation, showing a reasonable profile-reproducibility. (c) F vs Δ obtained as the average of the second to fifth tensile experiments from four different samples, showing a good reproducibility. (d) F vs Δ obtained by averaging results of four new-sample experiments (performed for sample 1 to 4) and by averaging results of the second to fifth tensile experiments performed on a single used sample, sample 4. In (a) to (d), $(h, d, w) = (2, 10, 50)$ in mm.

when stretched.

Accordingly, the curve obtained from new samples and those obtained from used samples are markedly different as shown in Fig. 2 (d). (In Figs. 3 and 4 below, the results for the new-sample experiment are given as an average of the curves obtained from 4 different new samples, whereas those for the used-sample experiment as an average of the curves obtained from the second to fifth extensions of a single used sample.) In the new-sample case, the force-extension curve shows a distinct peak with a sharp drop after the peak (although this feature tends to become less significant after averaging), which corresponds to the in-plane to out-of-plane transition. In contrast, in the used-sample case, the force-extension curve shows a moderate change of slope without a sharp drop near the end of the initial quasi-linear region.

B. Comparison with previous scaling laws

In recent studies, we have developed two models for the mechanics of the extension of kirigami. The first model [8] predicts a discontinuity of the force-extension ($F - \Delta$) curve, somewhat similar to the curve obtained from new samples shown in Fig. 2 (d). On the contrary, the second model [22] predicts a continuous $F - \Delta$, somewhat similar to the curve obtained from used samples shown in Fig. 2 (d). However, both models predict the same scaling laws for the spring constant K in the initial linear regime represented by the relation $F = K\Delta$ and the critical extension Δ_c at which the mechanical transition occurs and the

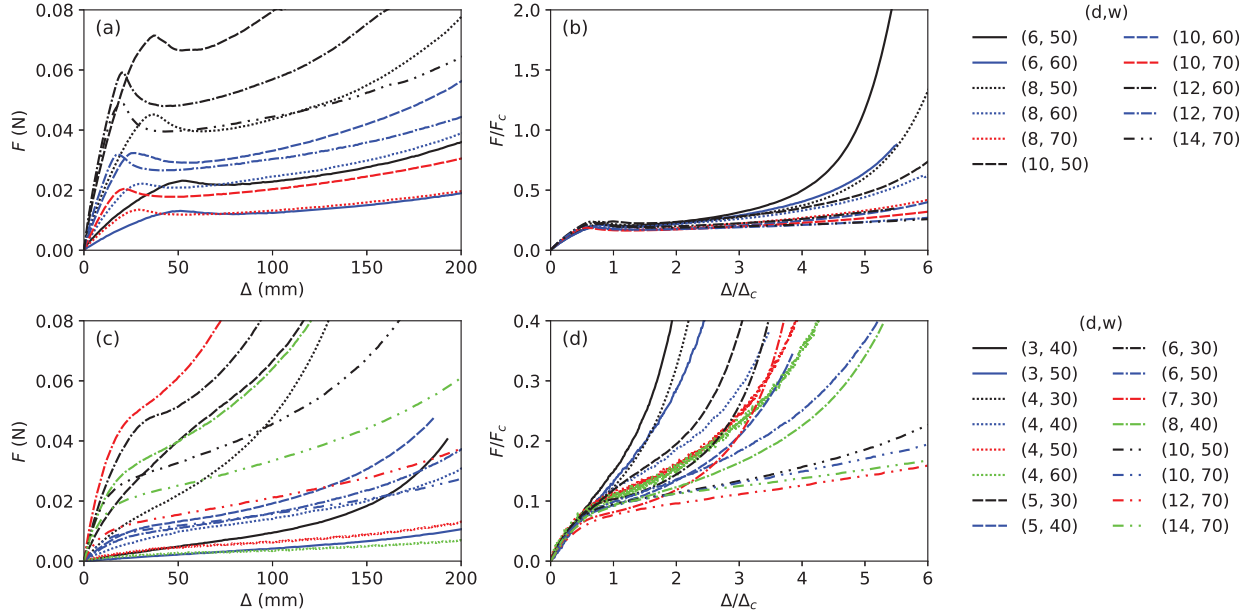


FIG. 3: (a) F vs Δ obtained from various new samples. (b) Data in (a) plotted using reduced axes. (c) F vs Δ obtained from various used samples. (d) Data in (c) plotted using reduced axes. Sample thickness h is 2.5 mm in (a) and 2.0 mm in (c). The parameters (d, w) are given in the legend in mm.

initial linear regime is terminated. The scaling laws are given in the forms

$$K = k/(2N) \text{ and } \Delta_c = 2N\delta_c, \quad (1)$$

with

$$k = c_1 E h (d/w)^3 \text{ and } \delta_c = c_2 h^2 / d, \quad (2)$$

where c_1 and c_2 are dimensionless numerical factors.

The coefficients were determined by comparing the theory and experimental data obtained from Kent paper (whose elastic modulus is much larger than in the present case) in [8] as

$$c_1/(2N) = 0.346 \pm 0.006 \quad (3)$$

$$c_2 = 3.02 \pm 0.05 \quad (4)$$

(We point out a small error in Fig. 3 b of [8]: the vertical axis is not $K_1/(Eh)$ but in fact $k_1/(Eh)$ and the line marked 'slope 3' represents $y = c_1 x^3$.)

We test the relevance of these relations, in our data, shown in Fig. 3. In (a) and (c),

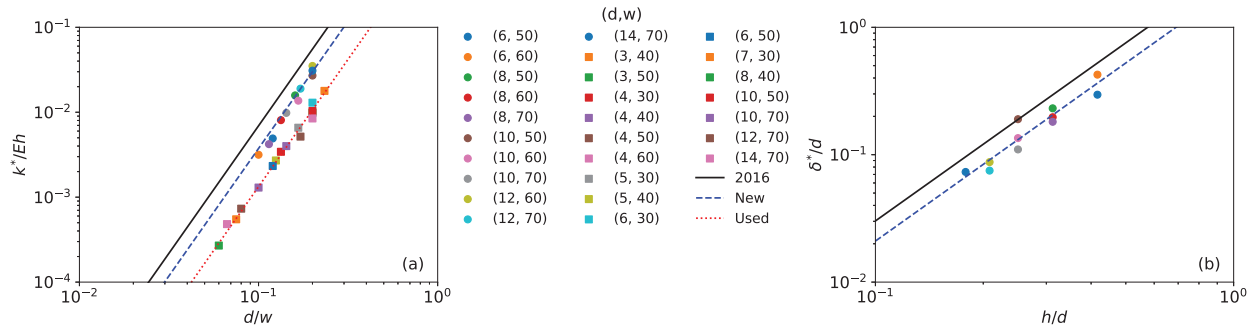


FIG. 4: (a) Reduced spring constant $K/(Eh)$ in the initial regime vs d/w . (b) Reduced critical extension Δ_c/d vs h/d . In (a) and (b), the data are obtained from the force-extension curve in Fig. 3 (a) or (c). The parameters (d, w) are given in the legend in mm, where circles and squares stand for the data obtained from the new- and used-sample experiments, respectively. (In (b), the data are shown only for the new-sample experiment. see the details for the text). The solid line are those fitting the data in Ref. [8]. The dashed and dotted lines are those fitting the data obtained in the new- and used-sample experiments, respectively.

the force-extension relation obtained from the new-sample and used-sample experiments are respectively given for various d and w . Note that those data were obtained with violating the condition of homogeneous deformation of elemental units that is assumed in deriving the two theories. In addition, in the used-sample experiment, all the elements possess small but finite initial rotating angles. This fact is also not reflected in previous theories and implies the absence of in-plane to out-of-plane transition in used samples.

To demonstrate the relevance of the previously obtained scaling laws, we renormalized the both axes F and Δ by characteristic force and extension given by $F_c = K\Delta_c$ and Δ_c , based on Eqs. (1) and (2) with the coefficients given in Eqs. (3) and (4). As a result, we surprisingly obtained clear collapses in both cases of the new- and used-sample experiments in the initial quasi-linear region, as shown in Fig. 3(b) and (d).

In Fig. 3(b) and (d), the collapsed linear region is not terminated at $(\Delta/\Delta_c, F/F_c) = (1, 1)$, which implies that numerical coefficients c_1 and c_2 are different from those given in Eqs. (3) and (4). In addition, while the terminal points of the linear region are located roughly at the same point $\Delta/\Delta_c = 0.7$ in Fig. 3(b), those points are scattered in the region around $\Delta/\Delta_c = 0.3$ to 0.7 in Fig. 3(d). This implies the following facts. (I) In the new-sample experiment, both of the scaling laws for k and δ_c in Eqs. (1) and (2) hold well with c_1 and c_2 different from those obtained in the previous work [8]. (II) In the used-sample experiment, the scaling law for k is highly relevant (with a different coefficient c_1) while that

for δ_c is only reasonably relevant.

To quantify the above remarkable features shown in Fig. 3(b) and (d), in Fig. 4 (a), we evaluated the slope K^* ($= k^*/2N$) of the initial linear regime of the $F - \Delta$ curve and plotted them on reduced axes, represented by k^*/Eh and d/w , because the first relation in Eq. (2) can be expressed as $k/Eh \simeq (d/w)^3$. As expected from a good collapse in Fig. 3 (b) and (d), we found K obtained from the data in Fig. 3 were described by the first relation in Eq. (2) on a highly quantitative level. The difference among the data obtained from kirigami made of paper [8], and those obtained from the present new- and used-sample experiments are only numerical factors $c_1/(2N)$ as indicated above, which are respectively given by Eq. (3), $c_1/(2N) = 0.187 \pm 0.007$ and 0.0665 ± 0.002 .

In Fig. 4 (a), as for the data obtained from the used-sample experiments, the collapse for k is distinctly clear and over a wide range. This is because the used-sample experiment overcomes difficulty in obtaining a good reproducibility, compared with the new-sample experiment, especially for small d and thus the used-sample experiment allows us to obtain meaningful data for a wide range of parameters.

In Fig. 4 (b), the validity of the second relation in Eq. (2) for the extension at the transition Δ_c is demonstrated for the new-sample experiment. For this plot, we evaluated the critical extension Δ^* ($= 2N\delta^*$) from the $F - \Delta$ curve, using the sharp peak position, in the new-sample experiment. The corresponding numerical factor c_2 is again different: the result $c_2 = 2.31 \pm 0.09$ for the present new-sample experiment differs from Eq. (4) obtained in [8]. Since the reproducibility of the new-sample experiment is not high even after averaging, the collapse observed in Fig. 4 (b) is less remarkable compared with that in Fig. 4 (a).

In the used-sample experiment, the in-plane to out-of-plane transition is absent due to the initial finite rotation angle of each element. Associated with this, the terminal points of the initial linear regime are scattered in Fig. 3 (d) as discussed above. In other words, the quantity Δ_c characterizes the end point of the initial quasi-linear regime, well in the new-experiment and reasonably well in the used-sample experiment.

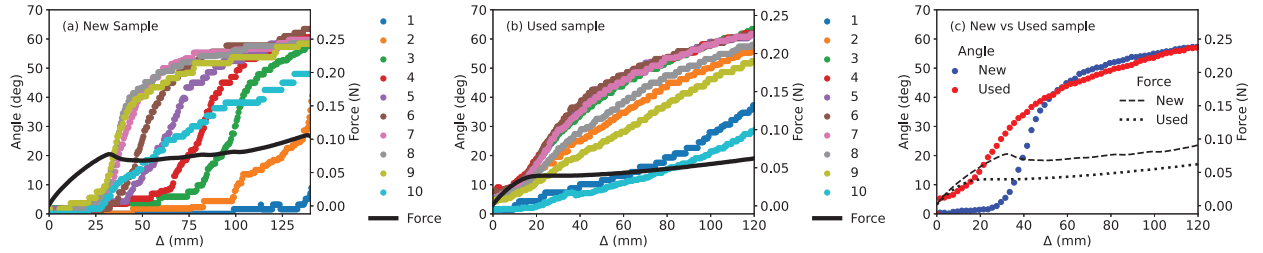


FIG. 5: (a) Angle θ vs extension Δ obtained for n th element in a single new sample, with the $F - \Delta$ plot. (b) Corresponding plot obtained in the used experiment for a single extension. (a) and (b) are obtained during the first extension of sample 3 in Fig. 2 (new sample with no averaging) and at the second extension of sample 1 in Fig.2 (used sample). The set (h, d, w) is $(2, 10, 50)$ in mm. (c) θ vs Δ shown as averages of the data for elements for which rotation starts earlier in the new-sample and used-sample experiment. See the text for the details on averaging.

C. Rotating angle and mechanical response

As already mentioned, we have developed two models: one disallows the coexistence of the in-plane and out-of-plane deformation and predicts discontinuous drop of force as a function of elongation at the transition point [8], and the other allows the coexistence and predicts continuous change of force at the transition [22]. In the latter work [22], we further consider the energy of kirigami as a function of the rotation angle, in which the rotation angle of each unit elements are assumed to be homogeneous: for a given elongation, all the unit elements rotate the same angle. As a result, in the continuous model, we found a striking similarity to the critical phenomena in thermodynamic phase transition [26, 27]: the energy as a function of the angle possesses a single minimum at $\theta = 0$ for small elongations but two minima at $\theta = \pm\theta_0(\Delta)$ for large deformations with $\theta_0(\Delta) \sim (\Delta - \Delta_c)^{1/2}$, which means

$$\theta_0(\Delta) \sim \begin{cases} 0 & \Delta \leq \Delta_c \\ (\Delta - \Delta_c)^{1/2} & \Delta > \Delta_c \end{cases}. \quad (5)$$

The theoretical structure is mathematically equivalent to Landau theory of the second-order transition, if we regard θ and $1/\Delta$ as the order parameter (such as the magnetization) and the temperature, respectively. In other words, the continuous model predicts a continuous change of the rotation angle with a critical exponent $1/2$ at the transition. On the contrary, we showed in [22] that the discontinuous model proposed in [8] exhibits a discontinuous jump of the angle at the transition point.

Motivated by these theoretical predictions, in Fig. 5 (a) and (b), we show results of

the measurement of the rotation angle θ of each elemental unit as a function of extension Δ , obtained in the new-sample and used-sample experiments, respectively, with the $F - \Delta$ relation superposed, although the present case is different from the theory in that the rotation angle is not the same for unit elements for a given Δ . In Fig. 5 (a) obtained from the new-sample experiment, corresponding to the observation for inhomogeneity in elemental-unit rotations mentioned earlier for Fig. 1 (c), as the elongation Δ increases the rotation starts from 7th to 9th elements (the other elements start rotating at larger values of Δ). In addition, the inflection point $\Delta = \Delta_{\text{inf}}$ (where the angle starts a sharp increase) on the $\theta - \Delta$ curves of such elements which start rotating "earlier" than the others roughly corresponds to the end point of the initial quasi-linear regime ($\Delta = \Delta_c$) on the $F - \Delta$ curve, which is superposed on the plot. Although elemental unit numbers for which the rotation start "earlier" (i.e., at a smaller Δ) depend on the sample, a good correlation between the inflection points $\Delta = \Delta_{\text{inf}}$ of such "earlier" $\theta - \Delta$ curves and the end point $\Delta \sim \Delta_c$ was a universal feature, regardless of the data obtained in the new-sample and used-sample experiments, as we can confirm in Fig. 5 (b).

In Fig. 5 (c), we show averages of the "earlier" $\theta - \Delta$ curves obtained in the new-sample and used-sample experiments using sample 1 to 4 discussed in Fig. 2, as specified below, with the force curves. For the new-sample experiment, we showed an average of the $\theta - \Delta$ profiles for the three "earlier" unit elements (i.e., three unit elements whose rotation start at the 1st to 3rd lowest values of Δ) of sample 1 to 4. For example, in Fig. 5 (a) obtained during the first extension of sample 3 (new sample), $n = 7, 8, 9$ are such three "earlier" unit elements. In other words, the average is taken over 12 profiles (3 profiles from each of 4 samples). For the used-sample experiment, we showed an average of the profiles for the three "earlier" unit elements of the second to fifth stretch (i.e., 4 stretches), all obtained from used sample 3 (the average is again taken over 12 profiles).

Figure 5 (c) thus obtained reveals the above-mentioned universal feature more clearly irrespective of whether the data are obtained from new or used samples: the inflection point $\Delta = \Delta_{\text{inf}}$ of the average of "early" $\theta - \Delta$ curve roughly corresponds to the end point $\Delta \sim \Delta_c$ of the linear regime of the $F - \Delta$ curve. In other words, the initial quasi-linear regime corresponds to the region in which the rotation angle are almost fixed and when rotation angle starts a sharp increase without jump (continuous increase) the force makes a transition into the second regime. This continuous change of the angle is consistent with

the continuous theory [22], which predicts a continuous change of the angle, rather than the discontinuous theory [8], which predicts a discontinuous jump (although the first derivative of θ with respect to Δ is continuous, which is different from the behavior of Eq. (5) at $\Delta = \Delta_c$).

However, the two averaged curves for the rotation angle obtained from new samples and those from used samples are clearly different, in that in the used-sample experiment the rotation angle starts from a finite value while in the new-sample experiment the angle starts from zero and increases sharply from a certain extension (transition point). Accordingly, the angle dependence on the extension in Eq. (5) obtained in the continuous theory [22] is very similar to the averaged the $\theta - \Delta$ curve obtained from new samples in Fig. 5 (c) except in the vicinity of the transition point, but different from the corresponding curve from used samples in Fig. 5 (c) in that the rotation angle before the sharp increase is a finite angle.

This finite angle before the sharp increase observed in the used-sample data implies a strong tendency of coexistence of the in-plane and out-of-plane deformations. As already suggested, in the continuous theory [22] we considered a general deformation in which the in-plane and out-of-plane deformations coexist (while such a coexistence is forbidden in the latter) and showed that the former contributes to the linear regime. In the used-sample experiment, the linear regime, which implies the existence of an in-plane deformation, is observed when the rotation angle is finite, which means the existence of a finite out-of-plane deformation: the in-plane and out-of-plane deformations coexist at a significant level even in the initial linear regime in the case of used samples.

IV. CONCLUSION

We examined mechanical response of a kirigami made of soft elastic sheets. Although the response was not highly reproducible for a new sample but fairly reproducible for used samples, we successfully quantify the response by focusing two types of averaged results: one for new samples and the other for used samples. We confirmed the existence of the initial linear regime in the force-elongation curve in both cases as in previous studies while the in-plane to out-of-plane transition, which is also a feature of previous study, was clearly observed only for the new-sample experiment. We surprisingly found previously obtained scaling laws successfully characterize the mechanical response although a number of assumptions in

previous theory such as homogeneity in rotation angle are violated and the elastic modulus is three orders of magnitude smaller in the present case, revealing universality of the mechanical response of kirigami. We further quantify the correlation between the response of rotation angle and that of force as a function of elongation to find the initial linear regime of the force-elongation curve corresponds to a quasi-plateau regime of the rotation-elongation curve and the linear regime ends when rotation starts in some of the elements. This tendency can be qualitatively interpreted in the light of a previous theory in which the coexistence of the in-plane and out-of-plane deformations is allowed. However, applicability of previously obtained scaling laws in the present case at a quantitative level is still a surprise. To understand this, we need further theoretical consideration. For example, in the present case, the effect of plastic deformation should be important, especially in the used-sample experiment, and thus, a quantitative theory including the effect of plastic deformation would be promising. We expect that the universal mechanical features revealed in the present study motivate future theoretical development and are useful for various applications.

Acknowledgements

This work was partly supported by JSPS KAKENHI Grant Number JP19H01859.

-
- [1] Koryo Miura. Method of packaging and deployment of large membranes in space. *The Institute of Space and Astronautical Science Report*, 618:1, 1985.
 - [2] Lizhi Xu, Terry C Shyu, and Nicholas A Kotov. Origami and kirigami nanocomposites. *ACS nano*, 11(8):7587–7599, 2017.
 - [3] Sicong Shan, Sung H Kang, Zhenhao Zhao, Lichen Fang, and Katia Bertoldi. Design of planar isotropic negative poisson’s ratio structures. *Extreme Mechanics Letters*, 4:96–102, 2015.
 - [4] Dennis M Kochmann and Katia Bertoldi. Exploiting microstructural instabilities in solids and structures: From metamaterials to structural transitions. *Applied mechanics reviews*, 69(5):050801, 2017.
 - [5] Katia Bertoldi, Vincenzo Vitelli, Johan Christensen, and Martin van Hecke. Flexible mechanical metamaterials. *Nature Reviews Materials*, 2(11):17066, 2017.

- [6] Melina K Bles, Arthur W Barnard, Peter A Rose, Samantha P Roberts, Kathryn L McGill, Pinshane Y Huang, Alexander R Ruyack, Joshua W Kevek, Bryce Kobrin, David A Muller, et al. Graphene kirigami. *Nature*, 524:204–207, 2015.
- [7] Zenan Qi, David K Campbell, and Harold S Park. Atomistic simulations of tension-induced large deformation and stretchability in graphene kirigami. *Phys. Rev. B*, 90(24):245437, 2014.
- [8] Midori Isobe and Ko Okumura. Initial rigid response and softening transition of highly stretchable kirigami sheet materials. *Scientific reports*, 6, 2016.
- [9] Aaron Lamoureux, Kyusang Lee, Matthew Shlian, Stephen R Forrest, and Max Shtein. Dynamic kirigami structures for integrated solar tracking. *Nature communications*, 6, 2015.
- [10] Yun Kyu Yi, Jie Yin, and Yichao Tang. Developing an advanced daylight model for building energy tool to simulate dynamic shading device. *Solar Energy*, 163:140–149, 2018.
- [11] Ahmad Rafsanjani and Katia Bertoldi. Buckling-induced kirigami. *Physical review letters*, 118(8):084301, 2017.
- [12] Doh-Gyu Hwang and Michael D Bartlett. Tunable mechanical metamaterials through hybrid kirigami structures. *Scientific reports*, 8(1):3378, 2018.
- [13] Ahmad Rafsanjani, Yuerou Zhang, Bangyuan Liu, Shmuel M Rubinstein, and Katia Bertoldi. Kirigami skins make a simple soft actuator crawl. *Science Robotics*, 3(15):eaar7555, 2018.
- [14] Ruike Zhao, Shaoting Lin, Hyunwoo Yuk, and Xuanhe Zhao. Kirigami enhances film adhesion. *Soft matter*, 14(13):2515–2525, 2018.
- [15] Terry C Shyu, Pablo F Damasceno, Paul M Dodd, Aaron Lamoureux, Lizhi Xu, Matthew Shlian, Max Shtein, Sharon C Glotzer, and Nicholas A Kotov. A kirigami approach to engineering elasticity in nanocomposites through patterned defects. *Nature Mater.*, 14:785–789, 2015.
- [16] Nan Hu, Dajing Chen, Dong Wang, Shicheng Huang, Ian Trase, Hannah M Grover, Xiaojiao Yu, John XJ Zhang, and Zi Chen. Stretchable kirigami polyvinylidene difluoride thin films for energy harvesting: Design, analysis, and performance. *Physical Review Applied*, 9(2):021002, 2018.
- [17] SH Chen, KC Chan, TM Yue, and FF Wu. Highly stretchable kirigami metallic glass structures with ultra-small strain energy loss. *Scripta Materialia*, 142:83–87, 2018.
- [18] Yichao Tang, Gaojian Lin, Shu Yang, Yun Kyu Yi, Randall D Kamien, and Jie Yin. Programmable kiri-kirigami metamaterials. *Advanced Materials*, 29(10):1604262, 2017.

- [19] Rujie Sun, Bing Zhang, Lu Yang, Wenjiao Zhang, Ian Farrow, Fabrizio Scarpa, and Jonathan Rossiter. Kirigami stretchable strain sensors with enhanced piezoelectricity induced by topological electrodes. *Applied Physics Letters*, 112(25):251904, 2018.
- [20] Yusuke Morikawa, Shota Yamagiwa, Hirohito Sawahata, Rika Numano, Kowa Koida, Makoto Ishida, and Takeshi Kawano. Ultrastretchable kirigami bioprobes. *Advanced healthcare materials*, 7(3):1701100, 2018.
- [21] Midori Isobe and Ko Okumura. Discontinuity in the in-plane to out-of-plane transition of kirigami. *Journal of the Physical Society of Japan*, 88(2):025001, 2019.
- [22] Midori Isobe and Ko Okumura. Continuity and discontinuity of kirigami’s high-extensibility transition: A statistical-physics viewpoint. *Physical Review Research*, 1(2):022001, 2019.
- [23] Y. Shiina, Y. Hamamoto, and K. Okumura. Fracture of soft cellular solids - case of non-crosslinked polyethylene foam. *Europhys. Lett.*, 76(4):588–594, 2006.
- [24] Yuki Kashima and Ko Okumura. Fracture of soft foam solids: Interplay of visco-and plasto-elasticity. *ACS Macro Lett.*, 3:419–422, 2014.
- [25] Atsushi Takei and Ko Okumura. Crack propagation in porous polymer sheets with different pore sizes. *MRS Communications*, pages 1–6, 2018; <http://dx.doi.org/10.1557/mrc.2018.222>.
- [26] John Cardy. *Scaling and renormalization in statistical physics*, volume 5. Cambridge Univ. Press, 1996.
- [27] Nigel Goldenfeld. *Lectures on phase transitions and the renormalization group*. CRC Press, 2018.